Design Considerations for the Design of Friction Pickers in Use for Runway Cleaning: An **Experimental Study**

Diaz Christofer^{®*}, Alvis Mario[®], Samo Luis[®], Silva Yuri[®], and Apaza Jorge[®]

Academic Department of Mechanical and Electrical Engineering, Universidad Nacional de San Agustín de Arequipa,

Email: cdiazar@unsa.edu.pe (D.C.); malvise@unsa.edu.pe (A.M.); lsamo@unsa.edu.pe (S.L.); ysilvav@unsa.edu.pe (S.Y.); japazagut@unsa.edu.pe (A.J.) *Corresponding author

Abstract—This study experimentally evaluates the design and performance of friction collector-based cleaning systems for the removal of Foreign Object Debris (FOD) on runways. A test rig was designed according to the guidelines established by the Federal Aviation Administration (FAA) circulars, including a variable speed strip simulating a category 5 concrete runway and optimized collector elements to maximize efficiency. Experimental results demonstrate that the system achieved greater than 90% FOD removal efficiency when operating at speeds in excess of 12.24 km/h (7.5 mph). This design introduces significant innovations in the configuration of the collecting elements and dynamic adjustment to varying operating conditions. The findings highlight its potential to improve aircraft safety, reduce maintenance costs and extend runway life at airports with high air traffic density.

Keywords—automated **Federal** Aviation cleaning. Administration (FAA), Foreign Object Debris (FOD), picker, runway

I. INTRODUCTION

The existence of FOD located on the runway represents one of the most common problems of any aeronautical center because they endanger the integrity of the aircraft during take-off and landing, opening the possibility of tragic accidents such as the most famous case of the Concorde in 2000 [1].

Foreign Object Debris (FOD) causes overloads on the undercarriage components of aircraft or, in some cases, is absorbed by engines, leading to a chain of destructive events. This occurs more frequently in some military aircraft because having air intakes at a relatively low height causes the airflow generated by the engine to absorb everything on the runway [2]. These objects can range from small metallic fragments to larger components, representing a latent risk to aviation safety. In any case, an encounter between an operational aircraft and a FOD is an event that is desired to be avoided.

To address this problem, personnel conduct a sweeping operation across the runway, a process known as a FOD WALK. This method is still used today and basically consists of many people walking along the runway searching for FOD [3]. The found FOD is discarded, and in some cases, when these are parts of an aircraft, a study is conducted regarding their origin. However, this manual method presents critical limitations:

- High dependence on human attention
- Vulnerability to staff distractions
- Impact of adverse weather conditions
- Low efficiency in exhaustive detection

This is why researchers are beginning to automate this process. Currently, there are technologies and systems responsible for keeping the runway clear of FOD, and the FAA has established a cleaning program that all created products follow. This program is divided into four areas, as shown in Fig. 1 [4].

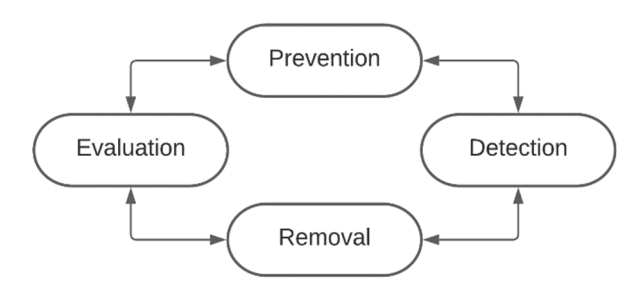


Fig. 1. Runway cleaning program [4].

However, most of these technologies primarily focus on detection, leaving a significant gap in efficient extraction processes. Recent materials science research highlights thermoplastic polyurethane (TPU) as an optimal solution for extraction components due to its temperature-resistant (≤90 °C) wear-resistant (0.12)properties [5]. The created systems comply with the mentioned program; for example, in Canada, the first system called QinetiQ Tarsier was installed, which uses

Manuscript received October 8, 2024; revised December 12, 2024; accepted April 8, 2025; published October 17, 2025.

radar and millimeter waves [6]; in Düsseldorf, Germany, iFerret is used, which is a system of optical electric sensors [7]; and in Tel Aviv, Israel, the Xsight Systems FODetect is utilized, which is a hybrid sensor with radar and optical technology [8]. All these products aim to locate the FOD on the runway, which are then extracted by personnel. Each system uses specific technologies that, although innovative, still maintain inherent limitations in their capacity for precise and efficient extraction.

Despite technological advancements, significant challenges persist in FOD extraction, especially in environments with budgetary or technological constraints. The gap between detection and extraction remains a critical unresolved issue. This program highlights two areas that are the steps taken during runway cleaning: detection and extraction. These two steps are continuous; first, the FOD is detected, and then it is extracted. This principle guides most of the systems created [9–11] as they focus on developing technology that detects FOD so it can later be extracted by personnel or a robot. However, a critical analysis reveals that the effectiveness of the process fundamentally depends on the precision of detection, making it a crucial link that is often suboptimized. Clearly, most systems created have addressed the detection step, and any other technology developed to detect FOD must meet the same expectations and standards proposed by the FAA [12]. However, the FOD WALK method is still used in environments where there is no capacity or budget to implement a detection system. To solve this, some airports where the advantages of detection systems are not necessary use systems that skip this step and focus on direct extraction [13–15].

Despite significant advances in FOD detection technologies, a critical gap remains in knowledge about efficient extraction systems, especially for friction collectors for airstrips. TPU-based collectors offer unique advantages through their microphase-separated structure (hard MDI-BDO/soft PTMG segments) that enables both debris capture and thermal stability [16]. Previous studies, primarily focused on earth movements and agriculture, do not consider the specific conditions of an aviation environment. Therefore, this research proposes a systematic method for designing friction collectors that improve FOD extraction, contributing an innovative methodology that can be implemented at Base Aérea N°4 of the Peruvian Air Force and potentially extended to other aviation contexts.

For extraction, the FAA indicates that there are various methods, including the following:

- 1) Mechanical systems
- a. Electric sweepers
- b. Vacuum systems
- c. Air jet blowers
- 2) Non-mechanical systems
- d. Friction carpet sweepers
- e. Magnetic bars
- f. Rough bands
- 3) Storage systems

Among these, non-mechanical systems are termed as such because they do not use any instrument of mechanical

or electrical power. Within this category, there is one in particular, due to its background in performing FOD extraction in very short times, the simplicity of operation, and the efficiency of the system in providing complete cleaning, known as the friction carpet sweeper [17]. This research experimentally studies the considerations needed to design friction collectors that originate from their principle of operation and are the main component of the mentioned friction carpet sweeper, with the objective of making them efficient when cleaning the runways of Base Aérea N°4 of the Peruvian Air Force (FAP), the environment where this study is focused and where cleaning and FOD requirements are generated. All this while providing a perspective focused on the analysis of rapid extraction on flat surfaces. The problem is the very limited amount of information related to the friction collector and the friction carpet, where only its commercial form is shown and not a design analysis. This creates a gap in research regarding important design parameters for these systems, such as shape, size, and movement speed, which complicates modeling and control of the friction collector. However, this collector shows similarities with the buckets of front-end loaders for earthmoving and some mechanisms for agriculture, so research in these areas is referenced to find insights about its structure and functioning to apply it to the friction collector. For example, the analysis of the forces encountered with a bucket in earthmoving is described in a study of wheeled electric loaders [18]. Energy efficiency and the relationship between the bucket's movement and the angle of attack with the materials it collects are studied in cable buckets [19]. On the other hand, in mechanisms for agriculture, the design of a bucket and the forces present when harvesting cassava in soil is studied, highlighting the dimensions and attack angle at the time of harvest [20]. Finally, studies on information collection reference the shapes of buckets in their attack zone, their uses, and their ergonomics during operation [21]. Nevertheless, despite having this information available, it is noted that these studies refer to the extraction and movement of large quantities of earth not related to FOD and in work soils not classified in the same way as in an aviation center. Consequently, there is a lack of studies addressing the design of collectors for use on runways. Therefore, the information from these investigations is utilized to some extent to relate it to the systematization that the FAA provides regarding the FOD that should be used for the study and about the types of runways that should be worked on.

The structure of the article is as follows. In Section II, the requirements of Base Aérea N°4 of the FAP, the study environment for the research, are analyzed. Section III presents the friction collector, its components, and its principle of operation. Section IV describes the test set and the study variables. Section V details the experimental tests and the results. Section VI shows the final result after testing a prototype designed based on the experimental studies. Finally, Section VII presents the final observations and conclusions.

II. ANALYSIS OF REQUIREMENTS FOR THE RUNWAY OF THE FAP AIR BASE

The analysis of the runway is based on the circulars proposed by the FAA, related to the physical evaluation [22] and the FOD prevention program that should be applied to it [23].

To start, the environment is evaluated because it is necessary to know the type of contact that the friction collector will have with the runway surface, as this determines the type of vibration the collector will experience. After analyzing the respective advisory circular titled AC 150/5320-17A Appendices A and B [22], it was established that the runway is divided into three zones, which are illustrated in Fig. 2.

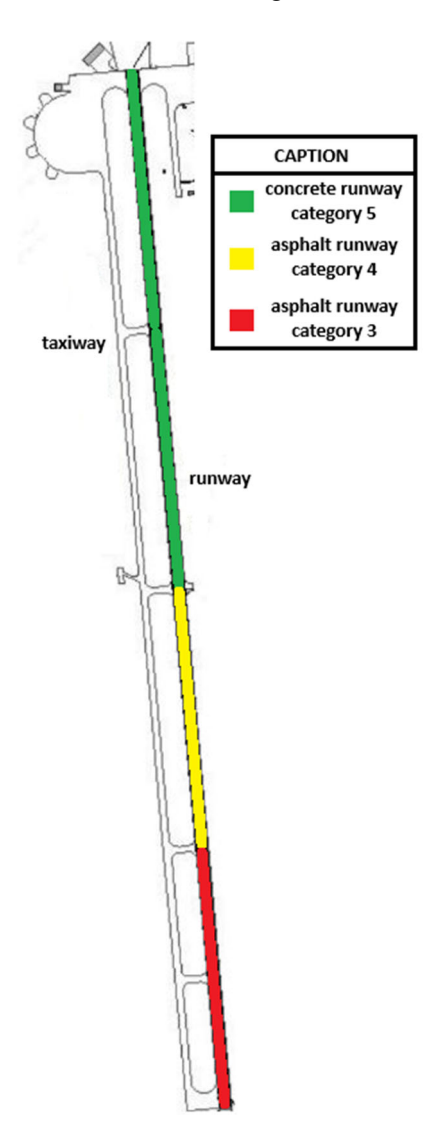


Fig. 2. Evaluation of the runway at base Aérea N°4 of the FAP.

Next, the zones of the runways are described according to the FAA as shown `in Fig. 2.

 Zone 1 (Green): Space that starts from the beginning of the runway up to 2,000 m in length. It is classified as a concrete runway category 5 since it does not present visible hazards and does not require any maintenance.

- 2. Zone 2 (Yellow): Space that starts from 2,000 to 3,000 m in length. It is classified as a category 4 asphalt runway since it presents slight scrapes, widely spaced and sealed cracks, some seals have leaks that require replacement at certain isolated points, and less than 10% of cracks need sealing.
- 3. Zone 3 (Red): Space that starts from 3,000 m to the end of the runway. It is classified as a category 3 asphalt runway since it presents thermal cracks spaced less than 10 feet apart where it is necessary to seal 25% of them and pavement settlements in cracks with less than 2.5 cm of depth.

With the evaluated runway, the FOD prevention program can be addressed. Using the respective advisory circular titled AC 150/5210-24A, the materials to be used for the tests were defined, which are proposed in a list by the FAA. To choose which of these materials to use, a consultation is made with the users of the runway, the Peruvian Air Force, indicating that the most common FOD are as follows:

- a. Bolts
- b. Nuts
- c. Washers
- d. Pieces of tire
- e. Deformed wires
- f. Asphalt

These FOD are illustrated in Fig. 3.

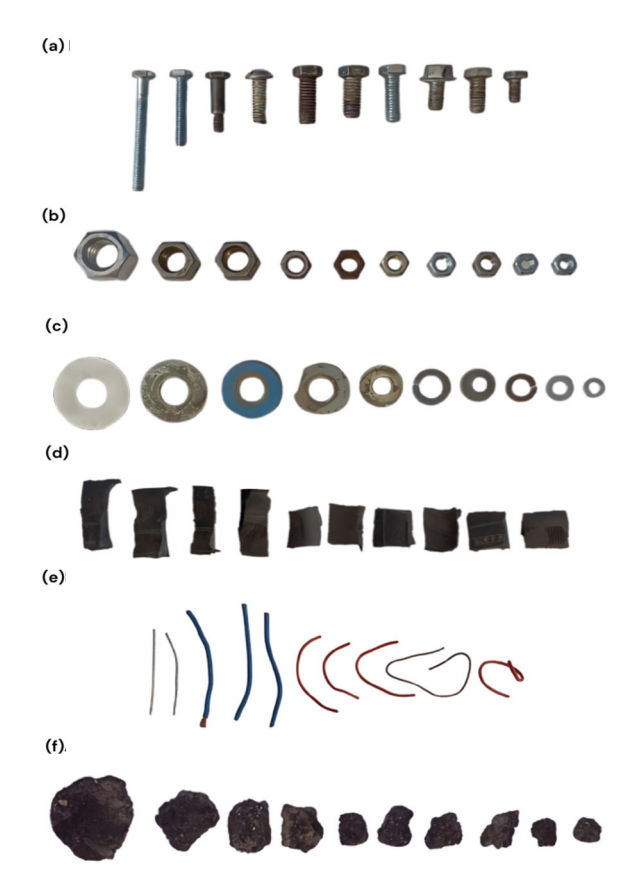


Fig. 3. FOD used for testing the prototype of the collector. (a) Bolt Testing; (b) Nuts Testing; (c) Washers Testing; (d) Tire Shreds Testing; (e) Deformed Wires Testing; (f) Asphalt Testing.

III. THE FRICTION COLLECTOR AND ITS COMPONENTS

The principle of extraction by friction consists of collecting the FOD that is reached by a collector while moving in a continuous direction, as described in Fig. 4. This principle, as shown in its commercial form Ref. [17], brings advantages such as simplicity in designing a functional collector, independence from processing systems, and high effectiveness while working. However, it also has requirements, such as the need for a drive element to provide the movement of the collector and the wear caused by the friction between the collector and the runway surface. The friction collector is the object used to collect FOD using the principle of friction collection, distinguished by four components that are shown in Fig. 5:

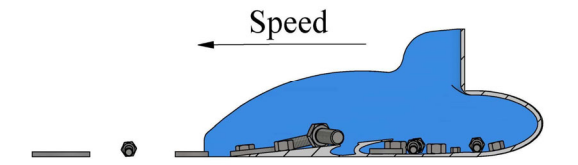


Fig. 4. Operating principle of the friction collector.

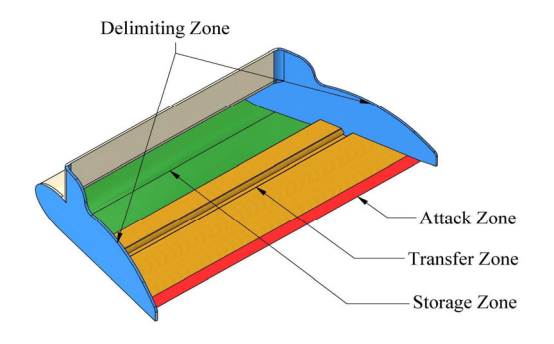


Fig. 5. The friction collector and its components.

The following describes the areas of the friction collector according to what is shown in Fig. 5.

- Attack zone: This component is the one that makes the first contact with the FOD. It must have a certain angle known as the attack angle to ensure that the FOD is collected and rises smoothly to the next component. Additionally, the attack zone defines the space in which the collector can operate.
- 2) Transfer zone: This component serves the function of moving the FOD to an area where it will not be affected by the vibrations caused by the movement of the collector. The transfer zone must have the necessary length to ensure that the FOD enters the area known as storage.
- 3) Storage zone: This component is where the FOD is stored after being collected and transferred by the previous components. The storage zone has an oval shape that prevents the FOD from exiting once it has entered due to vibrations.
- 4) Delimiting zone: This component temporarily prevents the FOD from falling out of the collector until it reaches the storage zone.

IV. STUDY VARIABLES AND CONFIGURATION OF THE TEST SETUP

In this chapter, the study variables of each component of the collector are presented, including an overview of the testing methodology and the design and configuration of the test setup. The objective of the tests is to determine the best values for the study variables of the collector when it operates in the extraction of FOD.

To simulate zone 1 of the runway, a BETA-C10SB type belt is used, designed to reach speeds of up to 15 km/h to replicate the impact of moving FOD on the collector, which is secured by accessories that prevent movement during the operation of the belt. The mentioned accessories also give the collector the ability to rotate about the rear axis to conduct tests with different parameters. The test setup is shown in Fig. 6.

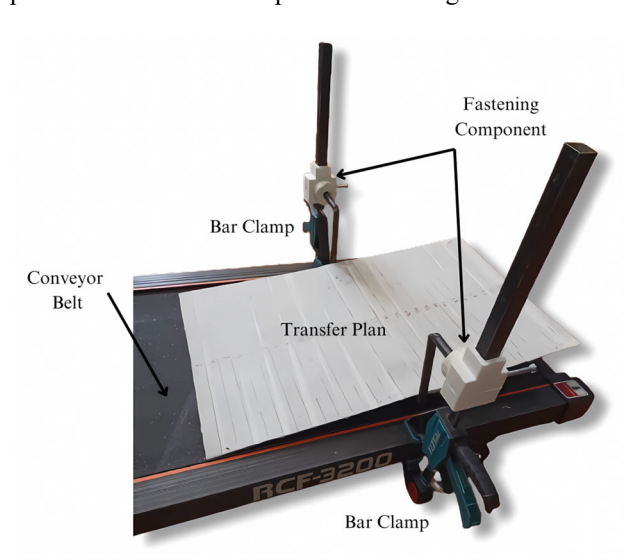


Fig. 6. Test setup of the experiment.

On the other hand, a variable is defined that affects all others related to the design of the collector, making it predominant. The operating speed is a variable that appears in the functioning of the collector and, together with the type of runway, causes the vibrations experienced by the collector. It is studied to determine the speed range where the efficiency of the collector is maximized. For this, speeds from 0 to 15 km/h are considered, and subsequently, cubic interpolation and extrapolation are performed to find the optimal speeds for each type of runway. Cubic interpolation is used because it models the performance variability of the tested materials in a smooth and continuous manner. This method, by fitting cubic polynomials between discrete data points, minimizes interpolation error and captures complex variations in the results. With the description of the environment and the predominant variable defined, the collector can be designed by components.

A. Attack Zone

The study variable of this component is defined as the attack angle. The attack angle is formed between the friction plane, which is the lower plane that makes constant contact with the runway surface, and the transfer

plane, which is the one that makes contact with the FOD (review Fig. 7).

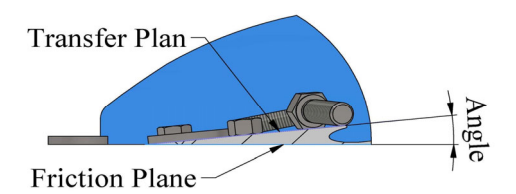


Fig. 7. Attack zone of the collector.

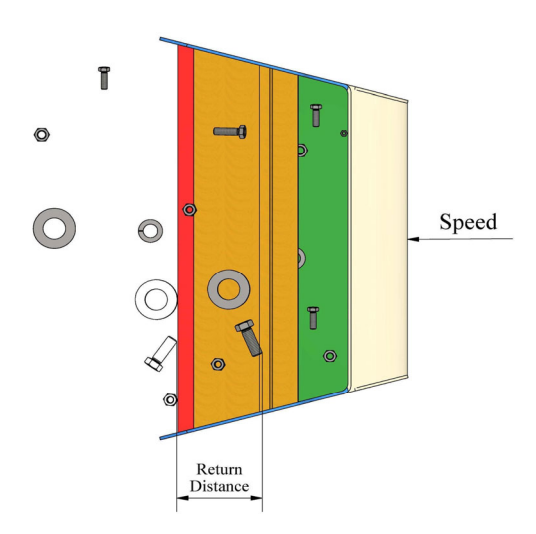
In the experimental methodology to study the attack angle, a 2 mm thick metal sheet is used along with the previously described test setup. The objective is to count the number of FOD that manage to rise onto the sheet after operating the treadmill at different speeds and causing the FOD to impact the metal sheet secured at different angles on the treadmill.

B. Transfer Zone and Storage Zone

The study variables of these components are defined as the return distance and the anti-return depth. The return distance is the distance that a FOD travels after entering the collector before it either returns or stays there (see Fig. 8(a)). The anti-return depth is the depth that the storage zone must have to prevent the FOD from returning or falling out once the return distance is reached, which is where the storage zone begins (see Fig. 8(b)).

In the experimental methodology to determine the return distance, the collector must be operated at the previously determined attack angle and at different speeds to see how much the FOD rises before returning. The data is interpolated using the same method as in the previous test, resulting in a behavioral trend for this parameter.

For the anti-return depth, experiments are conducted using the previously calculated variables, and Pmax is defined as the maximum depth that the storage zone can have at the studied angle and return distance. To achieve this, the FOD is placed inside the container, and the treadmill is activated to observe whether, after the vibratory movements caused by friction, the FOD stays in the storage zone. Table I summarizes the study variables of the collector.



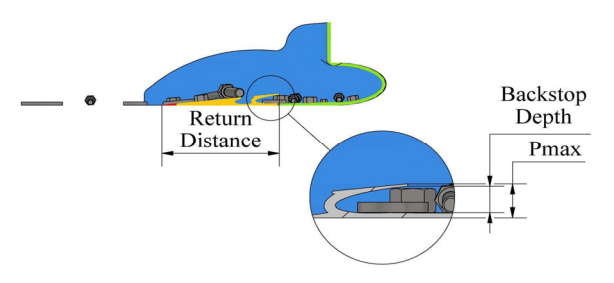


Fig. 8. Transfer and storage zone of the picker.

TABLE I. STUDY VARIABLES OF THE COLLECTOR

Component	Variable	Unit
Attack zone	Attack angle	degrees (°)
Transfer zone	Return distance	centimeter (cm)
Storage zone	Anti-return depth	millimeter (mm)

V. EXPERIMENTAL EVALUATION OF THE STUDY VARIABLES OF THE COLLECTOR

This section addresses the need to evaluate the collection and retention properties of the collector in an effort to define and adjust its design characteristics for future use.

A. Attack Zone

The experimental evaluation consists of operating the treadmill with the metal sheet placed on top and secured to the accessories. Initially, the belt is in operation, and the FOD are released at the beginning so that they gain speed and simulate the contact between the FOD and the collector correctly. The objective of the test is to count the number of FOD that manages to climb the sheet. As the tests are conducted, the attack angle varies between 2° and 18°, and the operating speed ranges from 0 to 15 km/h. Thus, this test finds the relationship between speed and attack angle, using the resulting efficiency for each test and for each different type of FOD, which includes waste such as plastics, metals, and paper as indicators. It is noteworthy that tests were performed with seven data points for each variable to later conduct cubic interpolation.

After conducting the tests, the results shown in Fig. 9 were obtained. The experimental results demonstrate that as the angle increases, efficiency tends to decrease, primarily due to the impact between the FOD and the inclined surface, which prevents the FOD from climbing the surface. For all types of FOD, it is observed that the slope of the efficiency and speed curves is greater at lower speeds and then decreases until reaching 0 when efficiency reaches 100%. This indicates that, in the case of certain lightweight items, not reaching 100% at 15 km/h will require a considerable increase in speed to achieve it; based on this assumption, the data is extrapolated, showing that the speed to achieve maximum efficiency with these items would be 19 km/h.

On the other hand, speed is a factor with very evident behavior, as it increases, efficiency also increases until it reaches a maximum of 100% and then remains at that peak, meaning that the attack angle remains unchanged. Once a minimum operating speed is reached, the collection of FOD is guaranteed. It is evident that there is a range of

speeds and attack angles where efficiency remains stable after reaching 100%; this range differs for each type of FOD and is presented in Table II. It is shown that some FOD, such as plastics, are easier to collect and require less speed, while others, like metals, require more effort. However, it is important to note that this does not indicate that angles outside the mentioned range will not achieve maximum efficiency; on the contrary, they do, but they require much more speed. Additionally, their behavior in some cases is difficult to visualize, as the slope mentioned earlier varies irregularly at these angles.

TABLE II. PARAMETERS TO ACHIEVE MAXIMUM AND STABLE COLLECTION EFFICIENCY FOR EACH TYPE OF FOD

FOD	Attack angle (°)	Speed (km/h)		
Bolts	<10	>8		
Nuts	<10	>11		
Washers	4–8	>19		
Tire shreds	<11	>13		
Deformed wires	<9	>13		
Asphalt	<12	>7		

In this context, the definition of "efficiency" refers to the proportion of FOD that is successfully collected compared to the total amount released. A standardized procedure was used to measure this efficiency, including manual counts and video recordings to verify the results. This approach ensures the validity of the obtained data.

The impact of the attack angle on efficiency can be attributed to the dynamics of FOD flow, where a steeper angle increases the risk of debris bouncing instead of adhering to the surface. It was also considered that consistency in executing the tests was crucial to ensure the repeatability of the results. Comparing these findings with previous studies shows a consistency in efficiency trends, providing a broader context for the results obtained. Finally, the practical implications of this study are relevant for optimizing the design of FOD collection systems in industrial environments, suggesting that adjustments in speed and angle could significantly enhance operational effectiveness.

This helps us understand the individual behavior of each type of FOD and indicates where greater attention should be focused. That said, it is evident that attention is directed toward achieving the collection of lightweight items, which have a very limited stability range. By ensuring the collection of these items, the collection of other FOD types is also guaranteed. To illustrate this, Fig. 10 is graphed to show the efficiency behavior at different angles and speeds.

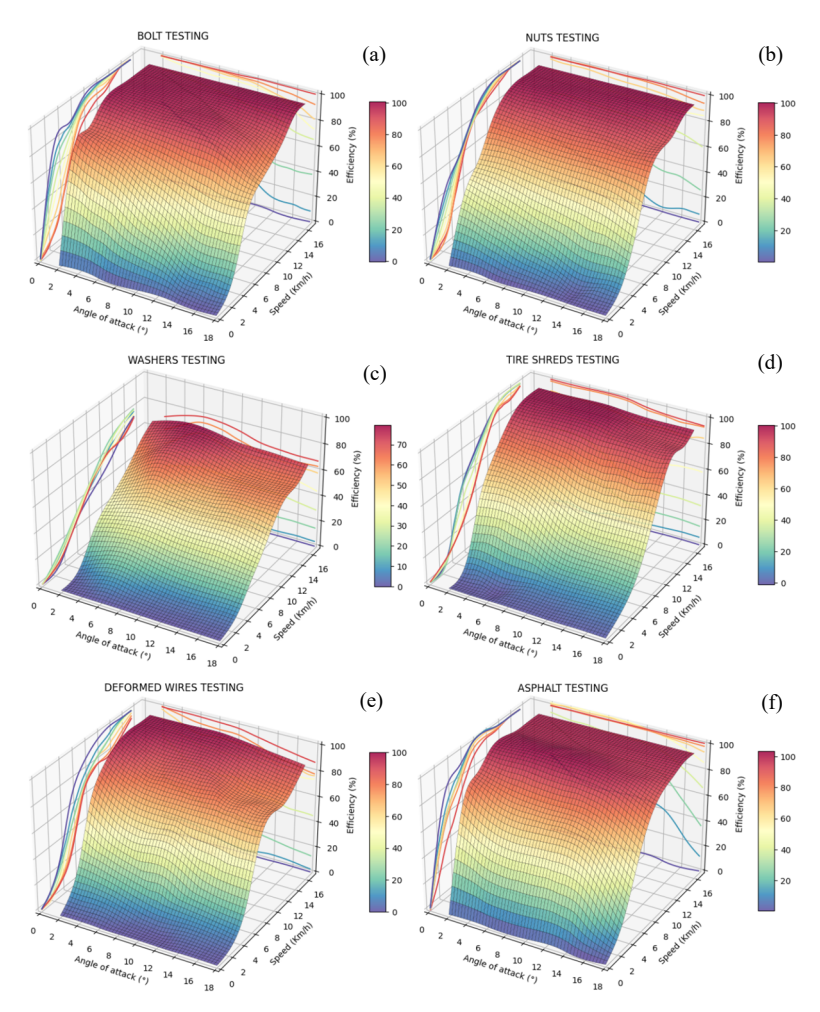


Fig. 9. Relationship between operating speed and angle of attack for different types of FOD. (a) Bolt testing; (b) Nuts testing; (c) Washers testing; (d)

Tire shreds testing; (e) Deformed wires testing; (f) Asphalt testing.

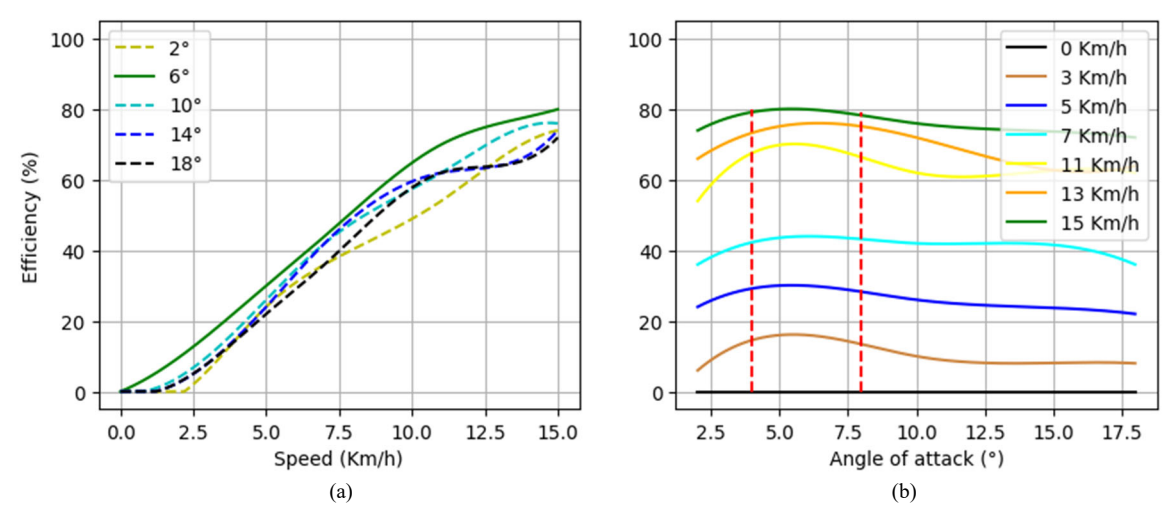


Fig. 10. Behavior of lightweight items at different attack angles and speeds. (a) Efficiency vs speed; (b) Efficiency vs angle of attack.

In Fig. 10(a), it is evident that speeds greater than 15 km/h are needed to achieve maximum efficiency, and that the curves at angles different from 6° exhibit irregular variations in their slope. On the other hand, Fig. 10(b) shows that angles below 4° and above 8° in tests with lightweight items cause a notable delay in reaching higher efficiencies, suggesting an optimal operating range. This acknowledges a key range of angles that should be addressed in subsequent tests; however, before analyzing further information about the collector, these results were first compared to the efficiency behavior when collecting different types of FOD simultaneously, which presents a more realistic scenario, and the results are graphed in Fig. 11.

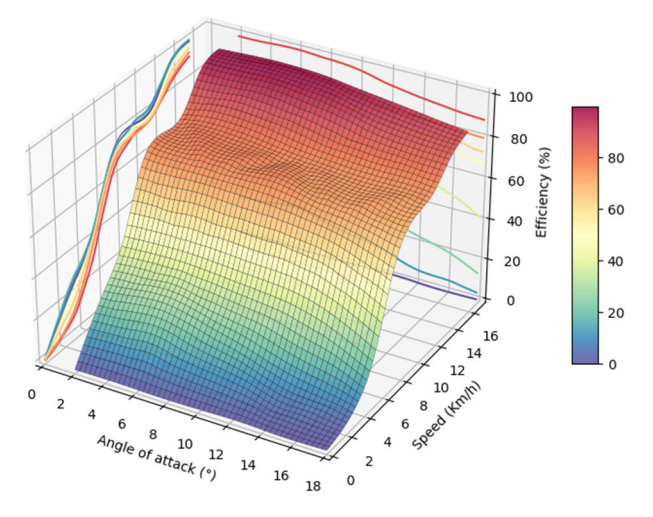


Fig. 11. Results of the tests for calculating the attack angle.

Due to the mix of FOD, a better efficiency is perceived at angles below 8°, and the speeds required to achieve maximum efficiency change from what was expected with lightweight items. It may seem that the results are unrelated, but this is due to the mix of FOD, as the

lightweight items were only 1/6 of the total FOD in the tests, and in a real environment, the proportion of FOD on the runway is unknown. To ensure the validity of the results, conditions during the tests were controlled, ensuring that the treadmill surface and the consistency in releasing the FOD were uniform. Therefore, an optimal efficiency threshold of 90% was used for analysis, as indicated in FAA circulars, which incorporates a range of possible failure. With this in mind, the graphs are expanded with key values to pinpoint values in our curves, as shown in Fig. 12.

After analyzing and evaluating the curves in Fig. 12(a) for different values, it was determined that the optimal range of attack angles remains between 4° and 8°, leading to the decision to use an angle of 6°. The speed analyzed at that angle, according to the curve in Fig. 12(b), indicates that the minimum required speed to achieve 90% efficiency when working with all combined FOD is 12.24 km/h. Finally, if different angles are desired in our collector, Fig. 12(c) shows the relationship between angles and speeds to maintain stable efficiencies. For example, the speed to reach the green curve, representing 90% efficiency with an attack angle of 6°, requires 12.24 km/h, and to achieve 100%, represented by the black curve, 13.79 km/h is needed.

An analytical approach was used to validate the results, including statistical significance analyses to evaluate data variability. The practical implications of using the identified optimal range of angles are relevant for the design of collection systems, suggesting that adjustments in speed and angle could significantly improve operational effectiveness. Additionally, a detailed understanding of the behavior of different FOD is considered essential for optimizing performance under real conditions. The graphs not only reflect quantitative results but also provide a clear view of how different parameters interact, which is crucial for future applications in the field of FOD collection.

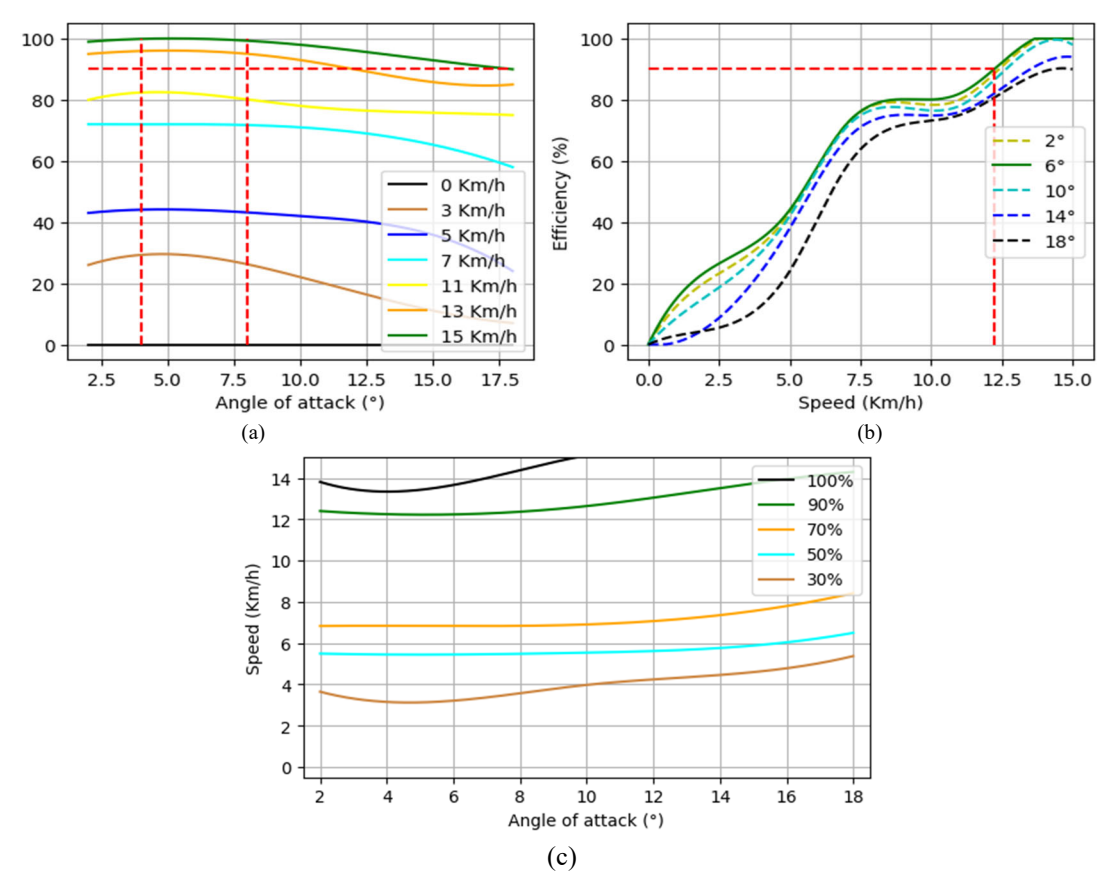


Fig. 12. Behavior of collection efficiency at different speeds and attack angles. (a) Efficiency vs angle of attack; (b) Efficiency vs speed; (c) Speed vs angle of attack.

B. Transfer Zone

For this experimental procedure, the treadmill will be operated in the same manner as in the evaluation of the attack zone. The objective of the test is to obtain the most frequent return distances for each type of FOD by only varying the speed of the treadmill, with the following values: 2.5, 5, 7.5, 10, 12.2, and 15 km/h. The experimental conditions were designed to capture a representative range of trajectories, with a segmentation of return distances between 0 and 60 cm, allowing for the evaluation of the dispersion dynamics of the materials in simulated scenarios.

This procedure aims to determine the maximum return distance and the optimal operating speeds needed to achieve 80% efficiency, thus enabling the appropriate dimensioning of the friction collector before designing it.

The selection of variables was based on technical and practical criteria, with the segmentation of the return distance allowing for the capture of representative trajectories considering factors such as variability in materials and the kinetic energy generated by the impact.

To extend the experimental results to speeds above 15 km/h, a linear regression was performed based on the means and standard deviations of the return distances obtained in the experimental range (2.5 to 15 km/h). This method allowed for the prediction of both the means and standard deviations of return distances at speeds of 17.4,

20, 22.3, 25, and 27.3 km/h. The linear regression equation used for each material took the form y = mx + b, where y represents the mean or standard deviation, x is the speed in km/h, m is the slope of the line, and b is the y-intercept, which are represented in Fig. 13. The specific results of the linear regressions for each type of FOD were as follows:

1. Bolts

Mean: y = 3.0661x - 8.2871, $R^2 = 0.9473$ Standard deviation: y = 0.915x - 0.4724, $R^2 = 0.8339$

2. Nuts

Media: y = 2.8364x-8.1481, $R^2 = 0.9573$ Standard deviation: y = 1.2564x-2.7654, $R^2 = 0.9699$

3. Washers:

Media: y = 1.6129x - 5.0588, $R^2 = 0.9304$ Standard deviation: y = 0.6699x - 1.695, $R^2 = 0.7822$

4. Tire shreds:

Media: y = 2.8219x-7.9056, $R^2 = 0.9304$ Standard deviation: y = 0.7472x-0.8875, $R^2 = 0.9474$

5. Deformed wires:

Media: y = 2.6791x-7.6061, $R^2 = 0.959$ Standard deviation: y = 1.382x-4.2719, $R^2 = 0.8938$

6. Asphalt:

Media: y = 2.1351x-3.2737, $R^2 = 0.9577$ Standard deviation: y = 1.1263x-2.1142, $R^2 = 0.9292$

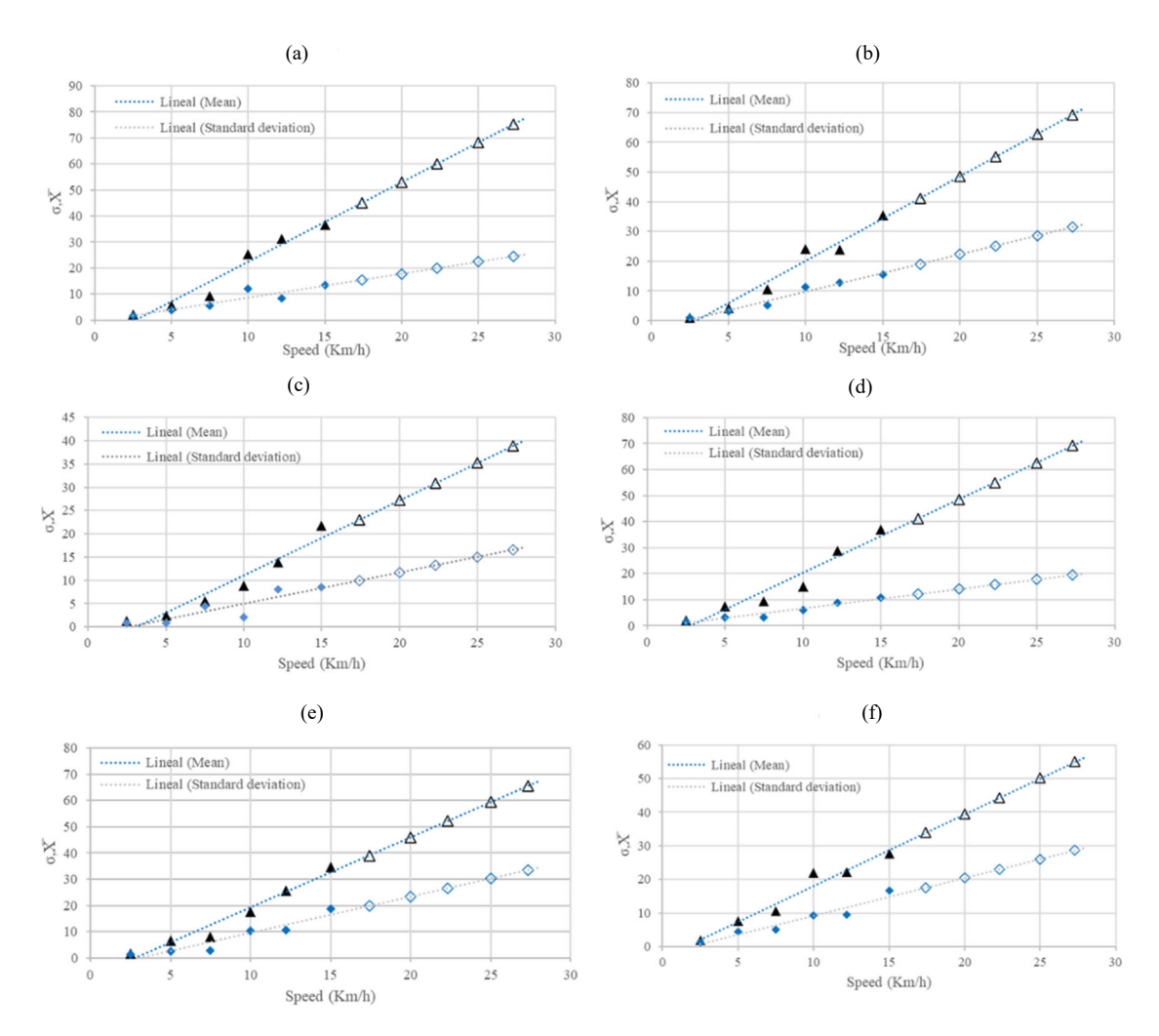


Fig. 13. Scatter plots with trend lines for data extrapolation above 15 km/h. (a) Bolt; (b) Nuts; (c) Washers; (d) Tire Shred; (e) Deformed Wires; (f) Asphalt.

After obtaining the experimental data, an analysis of the data was conducted, visualized in Fig. 14 and Table III. For bolts, the mean displacement significantly increases with speed, going from 2.23 cm at 2.5 km/h to 75.42 cm at 27.3 km/h. This increase can be explained by the higher mass and rigidity of the material, which responds more efficiently to applied forces at high speeds. However, this increase in displacements is accompanied by a considerable rise in the standard deviation, from 1.66 cm at 2.5 km/h to 24.51 cm at 27.3 km/h. This behavior reflects greater dispersion in the data, likely due to the accumulation of kinetic energy affecting the material's response.

The standard errors also support this observation, starting at 0.303 cm and increasing to 4.475 cm at 27.3 km/h, indicating that measurements become less precise at higher speeds. This increase in uncertainty may be attributed to variations in the material's behavior as speed increases.

Nuts exhibit similar behavior to that of bolts, with mean displacements increasing from 1.05 cm at 2.5 km/h to 69.29 cm at 27.3 km/h. However, the more compact shape of the nuts allows for a somewhat more controlled

displacement compared to bolts. Despite this, the standard deviation continues to rise considerably from 0.89 cm at 2.5 km/h to 31.53 cm at 27.3 km/h, indicating a greater degree of dispersion in the data as speed increases.

Standard errors also follow the same trend, starting at 0.162 cm and reaching 5.757 cm at 27.3 km/h, reflecting lower reliability of measurements at higher speeds, likely due to the more erratic behavior of nuts under greater kinetic energy.

For lightweight items, mean displacements also increase with speed, but the increase is more moderate. From 1.36 cm at 2.5 km/h, they reach 38.97 cm at 27.3 km/h. This behavior may be attributed to the lower density of the material and its greater resistance to displacement. The standard deviation also rises, from 0.74 cm at 2.5 km/h to 16.59 cm at 27.3 km/h, but less pronounced than in the other FODs, suggesting a more controlled response at higher speeds.

Standard errors remain relatively low compared to other materials, starting at 0.135 cm at 2.5 km/h and reaching 3.029 cm at 27.3 km/h. This indicates that measurements are more consistent for lightweight items, even at high speeds.

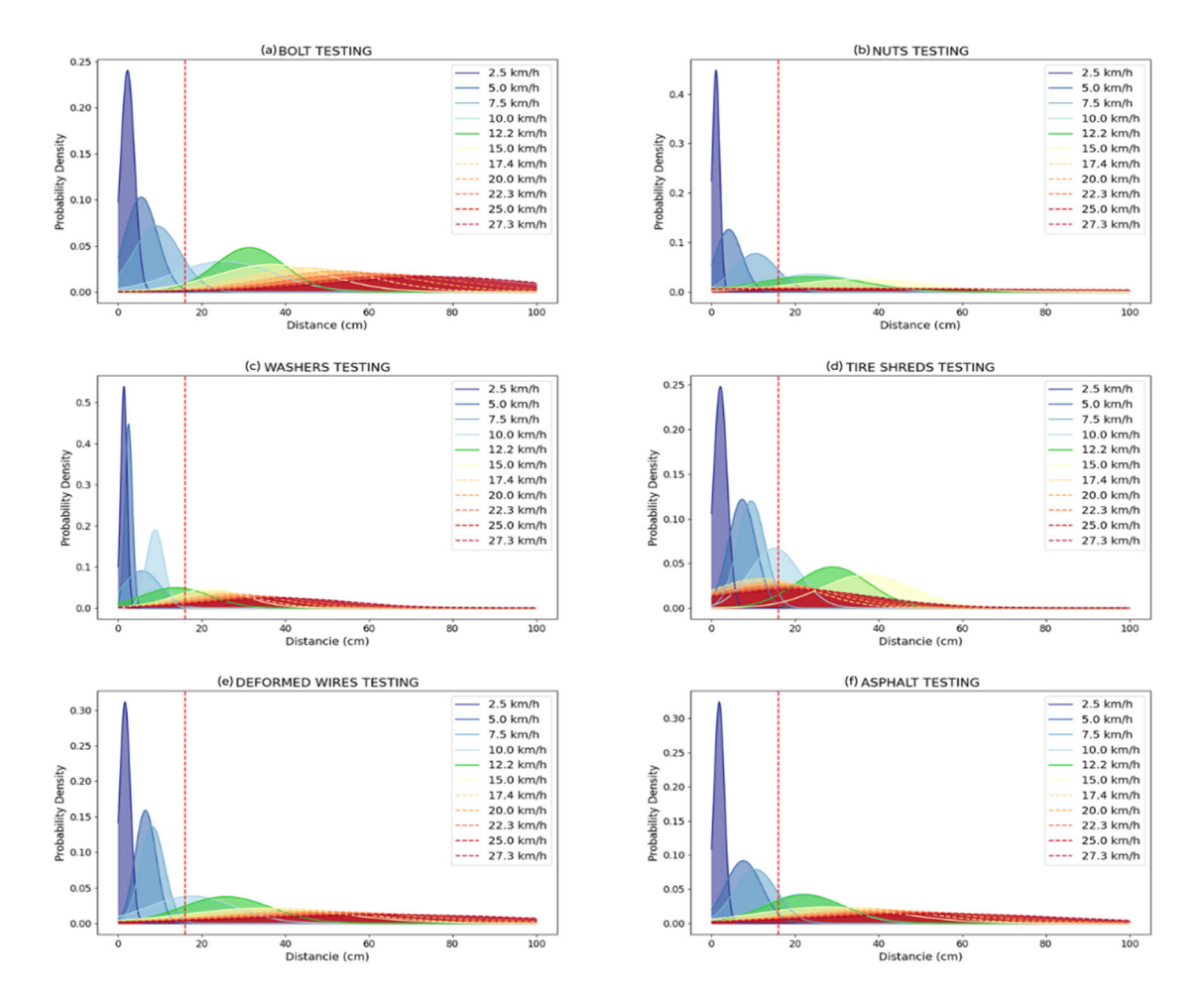


Fig. 14. Relationship between operating speed and return distance for each different type of FOD. (a) Bolt Testing; (b) Nuts Testing; (c) Washers Testing; (d) Tire Shred Testing; (e) Deformed Wires Testing; (f) Asphalt Testing.

TABLE III. CALCULATION OF MEAN, STANDARD DEVIATION, AND STANDARD ERROR

Bolt				Nuts			Washers			
Speed (Km/h)	Mean (cm)	Standard deviation	Standard error	Mean (cm)	Standard deviation	Standard error	Mean (cm)	Standard deviation	Standard error	
2.5	2.23	1.66	0.303	1.05	0.89	0.162	1.36	0.74	0.135	
5.0	5.48	3.88	0.708	4.12	3.16	0.577	2.45	0.89	0.162	
7.5	9.2	5.58	1.019	10.55	5.15	0.94	5.6	4.42	0.807	
10.0	25.37	12.06	2.202	24.13	11.28	2.059	8.83	2.10	0.383	
12.2	31.38	8.31	1.517	23.79	12.93	2.361	13.8	8.08	1.475	
15.0	36.67	13.44	2.454	35.53	15.58	2.845	21.8	8.57	1.565	
17.4	45.06	15.45	2.821	41.21	19.1	3.487	23.01	9.96	1.818	
20.0	53.03	17.83	3.255	48.58	22.36	4.082	27.20	11.70	2.136	
22.3	60.09	19.93	3.639	55.1	25.25	4.610	30.91	13.24	2.417	
25.0	68.37	22.4	4.09	62.76	28.64	5.229	35.26	15.05	2.748	
27.3	75.42	24.51	4.475	69.29	31.53	5.757	38.97	16.59	3.029	
C1		Tire shred	s		Deformed Wires			Asphalt		
Speed	Mean	Standard	Standard	Mean	Standard	Standard	Mean	Standard	Standard	
(Km/h)	(cm)	deviation	error	(cm)	deviation	error	(cm)	deviation	error	
2.5	2.1	1.61	0.294	1.61	1.28	0.234	1.82	1.23	0.225	
5.0	7.3	3.28	0.599	6.51	2.51	0.458	7.6	4.35	0.794	
7.5	9.47	3.33	0.608	8.13	2.93	0.535	10.52	5.06	0.924	
10.0	15.09	5.97	1.09	17.6	10.41	1.901	21.97	9.22	1.683	
12.2	28.91	8.69	1.587	25.76	10.62	1.939	22.15	9.58	1.749	
15.0	37.00	10.80	1.972	34.60	18.76	3.425	27.75	16.67	3.044	
17.4	41.2	12.11	2.211	39.01	19.77	3.609	33.88	17.48	3.191	
20.0	48.53	14.06	2.567	45.98	23.37	4.267	39.43	20.41	3.726	
22.3	55.02	15.78	2.881	52.14	26.55	4.847	44.34	23.00	4.199	
25.0	62.64	17.79	3.248	59.37	30.28	5.528	50.1	26.04	4.754	
27.3	69.13	19.51	3.562	65.53	33.46	6.109	55.01	28.63	5.227	

In tire pieces, the mean displacements increase significantly, from 2.10 cm at 2.5 km/h to 69.13 cm at 27.3 km/h. This increase can be explained by the material's elasticity and deformation capacity, which responds more dramatically to impact at high speeds. However, this increase in displacements is accompanied by a rise in standard deviation, from 1.61 cm at 2.5 km/h to 19.51 cm at 27.3 km/h. This behavior reflects greater dispersion in the data, possibly due to the irregular shape of the tire pieces, leading to more erratic movement.

The analysis of standard errors reinforces this conclusion, with values ranging from 0.294 cm at 2.5 km/h to 3.562 cm at 27.3 km/h. This indicates lower precision in measurements at high speeds, likely due to disorder and variability in the movement of the individual pieces.

For deformed wires, the means also increase significantly, going from 1.61 cm at 2.5 km/h to 65.53 cm at 27.3 km/h. However, due to their greater rigidity and irregular shape, the displacements are more erratic. The standard deviation increases from 1.28 cm at 2.5 km/h to 33.46 cm at 27.3 km/h, indicating that data dispersion is greater due to variations in the orientation and contact of the wires at the moment of impact.

Standard errors follow this trend, starting at 0.234 cm and increasing to 6.109 cm at 27.3 km/h. This reflects that measurements are less reliable at higher speeds, with greater data dispersion, possibly attributed to the flexibility and uneven shape of the wires.

The behavior of asphalt is more stable compared to the other materials. The mean displacements range from 1.82 cm at 2.5 km/h to 55.01 cm at 27.3 km/h, showing a moderate increase compared to the other FODs. This can be attributed to the greater rigidity of asphalt, which dissipates impact energy more evenly. The standard deviation also increases with speed, but to a lesser extent, from 1.23 cm to 28.63 cm.

Regarding standard errors, the values start low, from 0.225 cm at 2.5 km/h, and increase to 5.227 cm at 27.3 km/h, but to a lesser degree than with other materials. This suggests that measurements of asphalt are more reliable even at higher speeds.

The joint analysis of means, standard deviations, and standard errors reveals how the properties and geometry of each material influence their behavior at different speeds. Overall, both the mean and standard deviation of return distances increase with speed, suggesting that additional kinetic energy at higher speeds significantly impacts the dispersion of materials. Tire pieces and deformed wires exhibit more erratic behavior, with greater displacements and dispersion due to their elasticity and irregular shapes. In contrast, bolts and nuts present a more controlled response, although they also experience greater variations at high speeds, reflected in higher standard deviations and standard errors.

Asphalt, being more rigid and homogeneous, shows the most stable behavior, with lower dispersion and greater reliability in measurements at high speeds. This analysis highlights the importance of understanding each material's characteristics, as differences in their response can have crucial implications in applications where speed

and impact play an essential role in the design and safety of systems.

In Fig. 14(a), for bolts, it is observed that at low speeds (2.5 km/h), return distances vary from 0 to 5 cm. When the speed increases to 5 km/h, the return distance increases, ranging from 1 to 11 cm. At 7.5 km/h, the distances oscillate between 2 and 18 cm, while at 10 km/h, they reach up to 40 cm. The highest speeds, such as 12.2 and 15 km/h, show a significant increase, with distances reaching up to 60 and 90 cm, respectively. From the previous analysis, we see that bolts with a maximum return distance of 16 cm and speeds above 15 km/h ensure the passage of FOD to the storage zone, where collection will be secured.

In Fig. 14(d), it can be observed that tire pieces at 2.5 km/h exhibit return distances ranging from 0.5 to 5 cm. At speeds of 5 km/h, the distances oscillate between 6 and 10 cm. At 7.5 km/h, the distances reach up to 11 cm. At 10 km/h, the return distances increase significantly, varying between 11.3 and 14.8 cm. At speeds of 12.2 km/h, the distances reach up to 40 cm, and at 15 km/h, the highest observed return distances are up to 57.8 cm. The general trend suggests that speed significantly increases the return distances of tire pieces due to kinetic energy and the material's possible elasticity, which is why a maximum guaranteed return distance of 16 cm should be maintained, operating at speeds greater than 17.4 km/h.

In Fig. 14(e), we can see that metal pieces at 2.5 km/h generally exhibit low return distances, between 0 and 3 cm. At 5 km/h, the distances vary between 1 and 10.5 cm. At 7.5 km/h, the return distances reach up to 11.5 cm. At 10 km/h, the distances increase significantly, ranging from 1 to 30 cm. At speeds of 12.2 km/h, the distances reach up to 43.8 cm, and at 15 km/h, the return distances reach up to 57.8 cm.

The trend of increasing return distance with speed is evident, suggesting that metal pieces are significantly affected by kinetic energy, implying a need for a maximum return distance of 16 cm and speeds exceeding 15 km/h.

In Fig. 14(f), it is observed that asphalt pieces at 2.5 km/h exhibit return distances ranging from 1 to 4 cm. At speeds of 5 km/h, the distances reach up to 14.2 cm. At 7.5 km/h, return distances vary considerably from 3 to 19.3 cm. At 10 km/h, the return distances are higher, reaching up to 40.7 cm. At 12.2 km/h, the maximum observed distances are 38.7 cm, and at 15 km/h, the return distances reach up to 58.7 cm. The relationship between speed and return distance for asphalt pieces demonstrates a constant increase, indicating that kinetic energy at higher speeds significantly affects the return distance of this material. Therefore, to ensure collection, the collector must operate at more than 17.4 km/h and have a maximum return distance of 16 cm.

After analyzing the graphs, it can be seen that all the analyzed components show a clear pattern of increasing return distance with increasing speed. This behavior is primarily due to the increase in kinetic energy that each component acquires at higher speeds. Bolts and nuts, while similar in behavior, present variations in their return distances, likely due to differences in their shape and mass. Lightweight items and tire pieces show greater return

distances at high speeds, which may be related to the elastic properties of these materials. Metal and asphalt pieces, although stiffer, also exhibit significant increases in return distances with speed, highlighting the predominant influence of kinetic energy in these results.

To ensure the collection of more than 80%, it is necessary to have a maximum return distance of 16 cm and operate at speeds exceeding 15 km/h. Additionally, a high frequency of FOD with return distances from 0 to 5 cm indicates a large group of FOD that cannot scale the attack angle. To address this, it is necessary to implement a system that increases the kinetic energy of these items to improve the collection efficiency of the proposed system.

C. Storage Zone

In this experimental procedure, the treadmill was operated in the same manner as in previous evaluations to determine the efficiency of the storage zone by measuring its capacity to maintain the FOD once reached. In other words, in this methodology, the location of the storage zone is tested, and its efficiency is evaluated. Note that when testing the location of the storage zone, the efficiency of the transfer zone is tested. This test was performed at 6 speeds: 2.2, 5, 7.5, 10, 12.2, and 15 km/h, 10 FOD of each of the 6 types under study were used, 5 tests are performed for each type of FOD, resulting in 180 tests, which means that 1800 times the FOD were thrown on the treadmill. The picker was designed with the parameters presented in Table IV and is graphically illustrated in Fig. 15 for better visualization. It can be noticed that the front width is larger than the rear one, which is done in order to achieve a larger action area at the time of picking up. Note that the storage area is profiled considering the profile of the shovels of the front loaders used in earthmoving, since they have the same collection capacity. Purpose as the picker being designed. In addition, it is important to mention that the storage area was not constructed to a greater depth because it was limited to a thickness below. After performing the experiments, the results are presented in Fig. 16, which presents the results for the location of the storage area, and Table V presents the efficiency of the storage area. When analyzing the location of the storage zone, the efficiency of the transfer zone at different operating speeds was observed. As before, the same behavior was observed, and the higher the speed, the greater the efficiency.

TABLE IV. DIMENSIONS OF THE PICKER DESIGN

No.	Name	Dimension		
A	Dimensions of the picker design	390 mm		
В	Transfer zone Fig. 16(b)	From the attack zone to		
	Transfer zone Fig. 10(b)	160 mm		
C	Angle of attack Fig. 16(c)	6°		
D	Profile of the storage area Fig. 16(d)	With a height of 48.2 mm		
Е	Rear wall Fig. 16(e)	Located 40 mm from the		
	Real wall Fig. 10(e)	start of the transfer zone		
	Location of the center of the	At 40.6 mm from the		
F	circumference of the storage zone	beginning of the transfer		
	profile Fig. 16(f)	area		
G	Depth of the storage zone Fig. 16(g)	11.817 mm		
Н	Rear width Fig. 16(h)	307.4 mm		

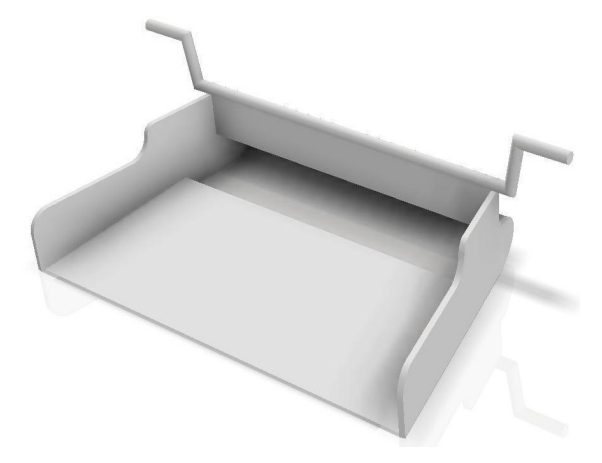


Fig. 15. Picker design.

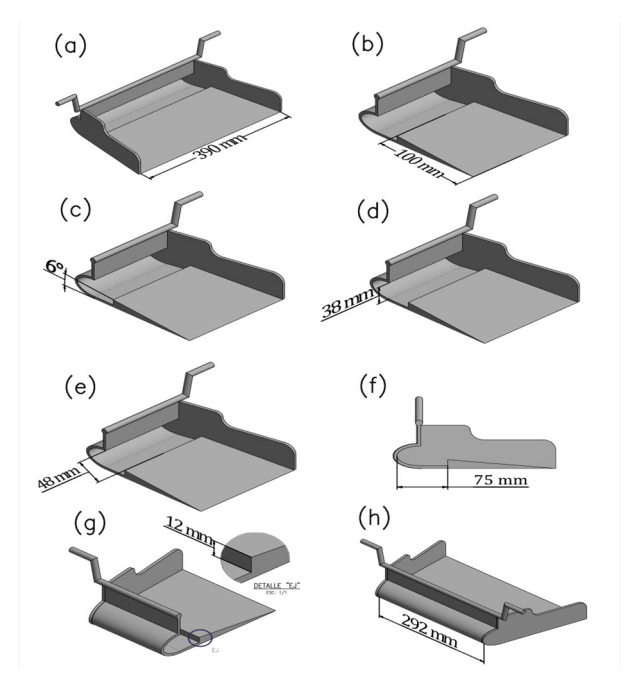


Fig. 16. Dimensions of the printed picker. (a) front width; (b) transfer zone; (c) angle of attack; (d) profile of the storage area; (e) rear wall; (f) storage zone profile; (g) depth of the storage zone; (h) rear width.

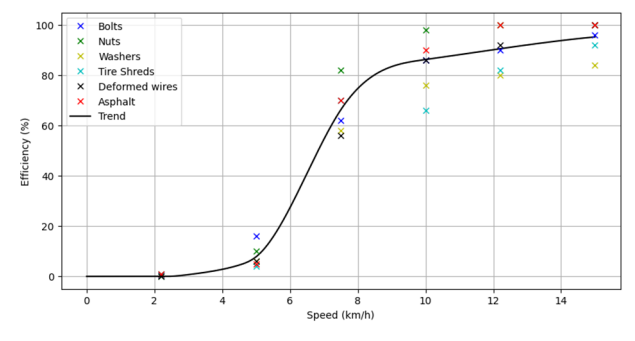


Fig. 17. Test results for the location of the storage area.

It should be noted that in these tests, interference of the storage zone profile was observed in the arrival of the FOD to the storage zone; i.e., of the 1800 FOD launched, 127 bounced off the rear wall, preventing them from entering the storage zone, representing 7% of the total. This implies

that the profile of the storage zone must be modified, which is a task performed in the next test. The results (Fig. 17) show that from 6 km/h the efficiency increases rapidly, reaching 66.45% at 7.5km/h. The trend shows that at 11.9 km/h, the efficiency reaches 90%, which means that from that speed onwards, the operation becomes allowed by international circulars.

Complementing this result and the idea that the higher the speed, the higher the efficiency, it appears in this graph that the margin of separation between the efficiencies of different FODs decreases as the speed increases. This generates safe knowledge from different friction picker use approaches. Since it is now assured that the location of the storage area is ideal, the behavior and efficiency of the FOD retention function can be analyzed. Here, Pmax is calculated as the maximum depth at which the storage area of the picker can be 16.817 mm. After this result, 5 mm is left as the bottom thickness of the storage area to support the friction loads of the picker, leaving the depth of the storage area at a distance of 11.817 mm. Table V presents the results of the tests.

It can be observed that the efficiency of the storage area is 100% or very close to this, which means that the depth provided to the storage area is ideal, considering that these data simulate a runway with a category 5 concrete surface.

In this way, the laboratory experiments were completed with the study parameters of each zone that made up the friction trough. This allows us to know the behavior of the friction trough.

TABLE V. STORAGE AREA EFFICIENCY

Speed (km/h)	Efficiency (%)
2.5	100
5	100
7.5	100
10	98
12.5	97
15	98

VI. EXPERIMENTAL EVALUATIONS IN A REAL ENVIRONMENT

In this section, the conjunction of all the design variables summarized in Table VI is carried out, evaluating the final picker in the real environment shown in Fig. 18, that is, in a runway evaluated as category 5 concrete. This environment coming from the tracks of the campus of the Universidad Nacional de San Agustín de Arequipa is delimited using safety cones with a distance of 300 m long by 3 m wide to drive a vehicle that serves as a movement to a mechanical assembly that holds the printed picker shown in Fig. 19. This vehicle, after pulling the dustpan by means of the mechanical assembly, passes over an area of 3 by 3 m, which is where the FODs used for this test are located (10 of each type of FOD under study), obtaining the results, i.e., the efficiency of the dustpan collection. It is important to highlight that for the tests, the FAA circular 150/5210-24 is applied to the environment but not to the speed suggestion because in the laboratory tests, maximum speeds of 15 km/h are reached,

and in the real environment tests, the same restriction is maintained.

TABLE VI. IMPORTANT PARAMETERS OF THE FRICTION PICKER

Parameter	Value	Description			
Amala of ottools	6°	Angle at which the picker impacts			
Angle of attack	O	the FOD			
Return distance	16cm	Distance at which the storage zone			
Return distance	100111	starts			
Depth of	11.817	Depth that ensures high			
storage zone	mm	containment of the FOD inside			
Material of	TPU	Theory about its atmestices			
manufacture		Throughout its structure			
Percentage of filler		Ideal percentage to maintain an			
	40%	elastic shape and avoid the			
	4070	hardness and brittleness of a higher			
		percentage			
Printing	Vertical	This direction is used to avoid			
direction	vertical	massive wear at the angle of attack			
Drinting datails	The pick	up is printed in 4 pieces and bonded			
Printing details	with Loctite 495 ethyl adhesive.				

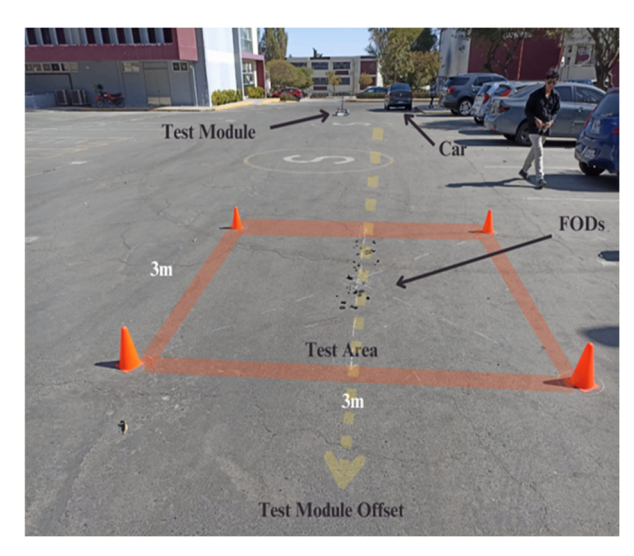


Fig. 18. Description of test area in real environment.

Fig. 20 shows the actual printed dustpan in its final form. With respect to the design of the printed dustpan, it is important to point out that the material used to print it is commercially available in the market, and it is used with the purpose of observing its durability when working under the friction loads caused by its operation. There is no experimental methodology for this material; it is only being put under observation.

The results are shown in Table VII, showing an efficiency of 93.6% for the friction scraper as a cleaning system. In which there is a high efficiency in the collection of tire and asphalt pieces, on the contrary case for the flips where there is a low efficiency compared to the other FOD. This may be due to its flat morphology, which causes little contact between the attack zone of the picker and the FOD, causing it to be necessary to take other options for a correct collection of the flips.

TABLE VII. TEST RESULT IN A REAL ENVIRONMENT

FOD			Total	Efficiency					
FOD	15	15	15	15	15	15	- I Utai	Linciency	
Bolts	10	9	10	10	9	10	58	96.7%	
Nuts	10	8	10	10	9	10	57	95%	
Washers	7	7	8	8	7	7	44	73.3%	
Tire shreds	10	10	10	10	10	10	60	100%	
Asphalt	10	9	9	10	10	10	58	96.7%	
Total	57	53	57	58	55	57	56.2	93.6%	
Efficiency	95%	88.3%	95%	96.7%	91.7%	95%	93.6%	Average	

The prototype's limitations include its working environment. Temperatures on runways can reach 40 °C to 90 °C. Since no experimental methodology exists for the collector material, working under constant friction loads not only causes wear in the impact area, but also overheats, causing the phenomenon of "thermal softening" when in contact with high-temperature surfaces. The working environment also presents small deformations or irregularities, such as elevations or openings, which prevent the collector from operating at its maximum efficiency.





Fig. 19. Real test module.



Fig. 20. Real friction picker.

VII. CONCLUSIONS

In this experimental study on the design of a friction collector for runway cleaning, the collector was divided into four zones: attack zone, transfer zone, storage zone, and delimiting zone. These zones were designed to ensure that Foreign Object Debris (FOD) effectively enters and remains stored within the collector after impact. The study variables were derived from each zone, except for the delimiting zone, which was based on bucket profiles used in earth-moving operations. The experimentation methodologies followed the guidelines outlined in the FAA advisory circular on FOD management. Following these guidelines, six common FOD types were selected for testing: bolts, nuts, washers, deformed wires, tire fragments, and asphalt pieces.

The design and test apparatus were built according to the FAA advisory circular for aerodrome pavement surface qualification at Air Base No. 4 of the FAP. The runway evaluation identified three distinct zones: category 5 concrete at the threshold, category 4 asphalt in the middle section, and category 3 asphalt in the final section.

A BETA-C10SB belt was used to simulate the collector's contact with the first zone surface. This belt, reaching speeds of up to 15 km/h, facilitated FOD impact testing while the collector was mounted on components providing rigidity and variable mobility.

For the attack angle variable, results showed that most FOD types require a low-angle approach to minimize resistance and facilitate upward movement. However, washers, being flat objects, require an angle between 4° and 8° for optimal collection efficiency, as the collector's thickness acts as a potential barrier. With an optimal attack angle of 6°, the minimum speed required to achieve a collection efficiency above 90% was determined to be 12.24 km/h.

Findings on the return distance variable revealed that, in general, higher speed improved collection efficiency for most FOD types. However, at speeds above 16 km/h, greater dispersion was observed, especially with deformable materials such as tire fragments and asphalt pieces, as well as with washers, which tend to bounce and resist collection due to their flat shape. To improve performance at higher speeds, design adjustments focusing on minimizing bounce and improving the guidance of problematic FOD toward the storage zone would be beneficial, possibly through additional damping elements or modifications to the collector's internal geometry.

The analysis of the storage zone, located 16 cm from the collector's leading edge, established that a minimum speed of 11.9 km/h is required to achieve 90% collection efficiency. Tests on the anti-return depth parameter revealed that a value of 11.817 mm offers nearly 100% efficiency, as the vibrations generated on category 5 concrete runways are insufficient to cause FOD to exit the storage zone once captured.

The prototype built based on these findings was tested in an environment similar to the study conditions, successfully maintaining the efficiency levels during preliminary testing. Overall, the collector demonstrated an average collection efficiency of 93.6%, meeting FAA recommendations.

Future research will focus on integrating this collector into a functional prototype for FOD removal at Air Base N° 4, complying with FAA regulations.

CONFLICT OF INTEREST

The authors declare no conflict of interest.

AUTHOR CONTRIBUTIONS

Diaz Christofer performed the reading and analysis of the state of the art as the FAA circulars to apply them to the runway and the realization of all the methodologies of the experimental tests, the definition and structuring of the

friction picker, the experimental tests, the analysis of the results as its presentation in the images and the writing of the article; Alvis Mario contributed to the design and manufacturing of the friction picker, created detailed illustrations for the article on the friction collector, conceptualized and designed test sets and participated in its construction with iterative improvements, conducted experimental tests, analyzed the results of the transfer zone section of the picker and the section on tests in a real environment, drafted the entire transfer zone section of the manuscript and developed graphical representations in the article; Samo Luis performed the design of the test set and the experimental tests; Silva Yuri facilitated the communications with the FAP allowing the development of the research; Apaza Jorge facilitated the necessary tools for the development of the experimental tests as the development of the research. All authors had approved the final version.

FUNDING

This work is part of the research project "PROTOTYPE OF A SEMIAUTOMATIC EQUIPMENT FOR CLEANING OES FROM THE FLIGHT TRACK", which has been funded by the Universidad Nacional de San Agustín de Arequipa under contract number PI-004-2023-UNSA.

ACKNOWLEDGMENT

The authors wish to express their deepest and sincerest gratitude to the Universidad Nacional de San Agustín de Arequipa for the invaluable support provided throughout this research. Their commitment and dedication have been fundamental for the development and success of this project. Also, they would like to thank all the facilities and support of the Communications and Electronics Squadron N*405 and Aeronautical Maintenance Squadron N*406 of Air Group N*4. Peruvian Air Force.

REFERENCES

- [1] Air France Flight 4590. (2015). Wikipedia. [Online]. Available: https://en.wikipedia.org/wiki/Air France Flight 4590
- [2] The FOD Control Corporation. (Nov. 21, 2022). The Essential Guide to Military FOD Prevention. [Online]. Available: https://www.fodcontrol.com/the-essential-guide-to-military-fod-prevention/
- [3] Federal Aviation Administration. (May 24, 2013). FOD resources.[Online]. Available: https://www.faa.gov/airports/airport_safety/fod/resources/
- [4] M. J. O'Donnell, Airport Foreign Object Debris (FOD) Management, Advisory Circular AC 150/5210-24, U.S. Dept. Transp., Fed. Aviation Admin., Washington, DC, USA, 2010.
- [5] Zhang et al., "High-temperature TPU for aerospace applications," Polym. Degrad. Stab., vol. 211, 109678, 2023.
- [6] QinetiQ's Tarsier system is cleared for take-off. (2012). [Online].
 Available: https://www.microwavejournal.com/articles/6243-qinetiq-s-tarsier-system-is-cleared-for-take-off

- [7] Stratech Systems Limited. (2012). Stratech's iFerretTM patent approved. Press Release. [Online]. Available: http://foddetection.com/wp-content/uploads/2011/05/Stratech-iFerret-Patent-Announcement-May19.pdf
- [8] Israel Airports Authority launches Xsight Systems' FODetect. (2017). Int. Airport Rev. [Online]. Available: https://www.internationalairportreview.com/news/1252 6/israel-airports-authority-launches-xsight-systems-fodetect/
- [9] G. Fizza, "Review on foreign object debris detection technologies and advancement for airport safety and surveillance," *Turk. J. Comput. Math. Educ.*, vol. 12, no. 3, pp. 1431–1436, 2021.
- [10] T. Chauhan, C. Goyal, D. Kumari, and A. K. Thakur, "A review on Foreign Object Debris/Damage (FOD) and its effects on aviation industry," *Mater. Today: Proc.*, vol. 33, pp. 4336–4339, 2020.
- [11] Y. Zhang, Z. Yan, J. Zhu, S. Li, and C. Mi, "A review of Foreign Object Detection (FOD) for inductive power transfer systems," eTransportation, vol. 1, 100002, 2019.
- [12] L. Werfelman. (May 2011). Clean sweep. Flight Saf. Found. [Online]. Available: http://flightsafety.org/asw/may11/asw_may1 1 p42-45.pdf
- [13] T. Rogoway and M. Méndez. (Apr. 16, 2015). This is how Russia cleans its aircraft carriers: with an aircraft engine and a tractor. *Gizmodo*. [Online]. Available: https://es.gizmodo.com/asi-limpiarusia-sus-portaaviones-con-un-motor-de-avio-1698168041
- [14] The FOD Control Corporation. Magnetic Sweepers.

 The FOD Control Corporation. [Online].

 Available: https://www.fodcontrol.com/product-category/magnetic-sweepers/
- [15] The FOD Control Corporation. (Nov. 11, 2022). TracSweep® Traction-Powered Debris Sweeper. [Online]. Available: https://www.fodcontrol.com/tracsweep/
- [16] H. Kim *et al.*, "Friction-Tailored TPU via microphase engineering," *Tribol. Int.*, vol. 185, 108112, 2024.
- [17] The FOD Control Corporation. (Feb. 20, 2023). FOD-Razor® Sweeper System. [Online]. Available: https://www.fodcontrol.com/fod-razor/
- [18] J. Wei, J. Zhao, and J. Wang, "Research on shovel-force prediction and power-matching optimization of a large-tonnage electric wheel loader," *Appl. Sci.*, vol. 13, no. 24, 13324, 2023.
- [19] J. Wu, G. Wang, Q. Bi, and R. Hall, "Digging force and power consumption during robotic excavation of cable shovel: experimental study and DEM simulation," *Int. J. Min. Reclam. Environ.*, vol. 35, no. 1, pp. 12–33, 2021.
- [20] L. Yulan, S. Youpan, L. Ye, F. Junqin, Y. Chenyu, and W. Tao, "A kind of digging shovel of cassava harvester design," in *Proc. Int. Conf. Digit. Manuf. Autom.*, Dec. 2010, vol. 1, pp. 34–38.
- [21] A. Freivalds, "The ergonomics of shovelling and shovel design—A review of the literature," *Ergonomics*, vol. 29, no. 1, pp. 3–18, 1986
- [22] Federal Aviation Administration (FAA). Airfield Pavement Surface Evaluation and Rating Manuals, Advisory Circular AC 150/5320-17A, U.S. Dept. Transp., Washington, DC, USA. [Online]. Available: https://www.faa.gov/airports/resources/advisory_circulars/index.cfm/go/document.information/documentID/1025586
- [23] Federal Aviation Administration (FAA). Airport Foreign Object Debris (FOD) Management, Advisory Circular AC 150/5210-24A, U.S. Dept. Transp., Washington, DC, USA. [Online]. Available: https://www.faa.gov/airports/resources/advisory_circulars/index.cfm/go/document.current/documentNumber/150_5210-24

Copyright © 2025 by the authors. This is an open access article distributed under the Creative Commons Attribution License which permits unrestricted use, distribution, and reproduction in any medium, provided the original work is properly cited (CC BY 4.0).